

Rolling friction in a linear microactuator

R. Ghodssi and D. D. Denton

*Department of Electrical and Computer Engineering and Materials Science Program,
University of Wisconsin-Madison, Madison, Wisconsin 53706*

A. A. Seireg

Mechanical Engineering Department, University of Wisconsin-Madison, Madison, Wisconsin 53706

B. Howland

Madison, Wisconsin 53705

(Received 30 September 1992; accepted 1 February 1993)

In order to design a precise and repeatable microelectromechanical system, friction and wear must be minimized in the surfaces of the microstructure. Rolling bearings are known to exhibit lower friction over sliding contact bearings in precision macromechanical systems. Rolling friction can be characterized on a microscale to facilitate the design of precision microelectromechanical systems. We have designed a test specimen utilizing stainless steel microballs (285 μm in diameter) in contact with silicon micromachined *v*-groove surfaces (310 μm wide, 163 μm deep, 10 000 μm long). Different thin films are deposited on the surface of the silicon *v* grooves and their frictional properties are investigated experimentally. We have shown that at zero applied normal force, the adhesion is dominant and as the applied normal force is increased, the friction coefficient reaches an asymptotic value below 0.01. The measured frictional forces represent the total resistance at the onset of rolling motion for the bearing which is generated at all the contacting surfaces. The measured values for the coefficient of friction will allow designers to select optimum lubricant surfaces to be used in microroller bearings using microballs and silicon micromachined V-groove surfaces.

I. INTRODUCTION

The design and optimization of microelectromechanical systems (MEMS) requires a basic understanding of the mechanical properties of materials used therein. Friction and wear on a microscale are two of the major factors that need to be thoroughly investigated in order for MEMS to operate more efficiently.

Tai and Muller¹ studied the dynamic coefficient of friction in a variable-capacitance integrated circuit (IC) processed micromotor. Friction coefficients in the range of 0.21–0.38 for silicon nitride-polysilicon surfaces were reported.¹ Lim *et al.*² used a polysilicon microstructure to characterize static friction. They reported friction coefficients of 4.9 ± 1.0 for coarse grained polysilicon-polysilicon interfaces and 2.5 ± 0.5 for silicon nitride-polysilicon surfaces. Mehregany, Senturia, and Lang³ measured both friction and wear using a polysilicon variable-capacitance rotary harmonic side-drive micromotor. They report a frictional force of $0.15 \mu\text{N}$ at the bushings and $0.04 \mu\text{N}$ in the bearing of the micromotor. Both the bushings and bearing surfaces were made of heavily phosphorus-doped polysilicon. Noguchi *et al.*⁴ examined the coefficient of maximum static friction for various materials by sliding millimeter-size movers electrostatically. The value obtained (0.32) for the static friction coefficient of silicon nitride and silicon surfaces in contact is smaller by a factor of 8 than the one reported by Lim *et al.*² However, the measured values for the dynamic coefficient of friction are close to those reported in Ref. 1.

Suzuki *et al.*⁵ compared the friction and wear of differ-

ent thin films by applying them to riders and disks of macroscopic scale and sliding them under the same loading conditions. Larger values of the dynamic coefficient of friction (0.7–0.9) were obtained for silicon nitride and polysilicon surfaces than the ones reported by Tai and Muller.¹ Deng and Ko⁶ examined the static coefficient of friction for different silicon compounds in a high vacuum chamber and under exposure to humidity and different gases. They observed that an exposure to oxygen gas increases the static coefficient of friction between the silicon compound mechanical contacts while an exposure to nitrogen gas often decreases it. A number of the values for sliding friction reported in the literature seem excessively large. This study was undertaken to evaluate the frictional resistance at the onset of rolling in microroller bearings and to provide a basis for comparison.

The mechanical properties of rolling element bearings in micromechanical systems have not yet been thoroughly investigated. Rolling element bearings are expected to be extensively used in MEMS because of their lower frictional properties, improved lifetime and higher stability in carrying loads when used in a microactuator. We have designed and built a test specimen and measurement system to investigate the rolling friction and wear of different materials on a microscale. Stainless-steel microballs are used to minimize friction between two silicon micromachined *v*-groove surfaces. The values of the start-up coefficient of friction of different thin films will be used to determine the best materials to be used as a solid lubricant to reduce the driving force necessary to move a linear microactuator.

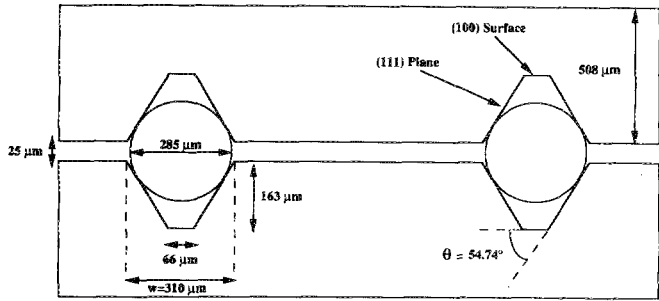


FIG. 1. Schematic representation of the cross-sectional view of the test specimen. Dashed lines show the width of the etched V groove (w) and the angle θ between the (100) surface and (111) plane.

II. EXPERIMENT

A. Test specimen

The test specimen is a parallel plate linear displacement element made of silicon micromachined V grooves with stainless-steel microballs in between. Figure 1 shows the cross-sectional view of the test specimen. The 54.74° angle is imposed by the crystalline structure of the silicon substrate and cannot be varied by using this micromachining technique. The use of a 54.74° angle, rather than the standard 45° angle, yields higher contact stress and large differential slip which may lead to an increase in friction coefficient for the rolling elements reported here. Figure 2 shows the top view of the parallel plates. The V grooves are $163 \mu\text{m}$ deep, $10\,000 \mu\text{m}$ long, $310 \mu\text{m}$ wide, and $14\,000 \mu\text{m}$ edge to edge. The stainless-steel microballs are $285 \mu\text{m}$ in diameter and positioned on the surface of the etched V grooves. This results in a uniform gap of approximately $25 \mu\text{m}$ between the silicon parallel plates. The stainless-steel microballs were obtained commercially.⁷ Different thin films were deposited on the surface of the silicon micromachined V grooves and the coefficient of friction between the deposited material and the stainless-steel microballs at the onset of movement was measured.

The silicon micromachined V grooves are made using 3 in., $0.1 \Omega \text{ cm}$ (100) p -type silicon wafers $508 \mu\text{m}$ thick. The wafers were cleaned using a standard RCA procedure. A thin layer (700 \AA) of thermal oxide was grown at 925°C . A 3000 \AA low-pressure chemical vapor deposition (LPCVD) silicon nitride was deposited on the thermal oxide. The samples were patterned photolithographically.

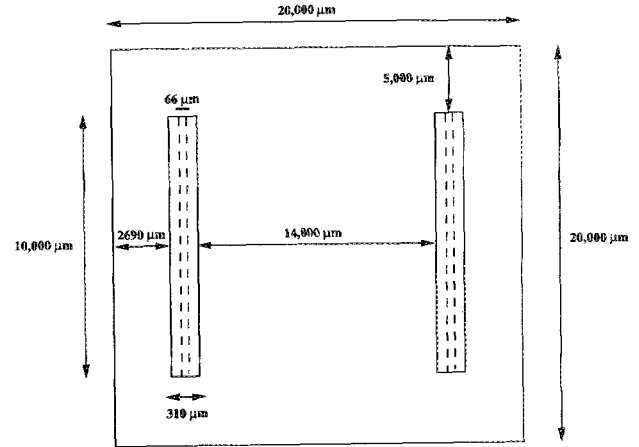


FIG. 2. Top view of the parallel plates. Each plate contains two V grooves. Dashed lines show the dimensions of the bottom of the V grooves.

A plasma etch (CF_4/O_2) was used to etch the silicon nitride and thermal oxide to form the anisotropic etch mask. The photoresist was removed using a chemical resist remover. The samples were then cleaned in a solution of $\text{NH}_4\text{OH}:\text{H}_2\text{O}_2:\text{H}_2\text{O}$ 1:1:6 in an ultrasonic bath for 5 min. Prior to micromachining, the samples were put in a dilute HF bath for 10 s to remove the native oxide. The patterned samples were immersed in a quartz reflux system containing an anisotropic etchant solution of $\text{KOH}:\text{H}_2\text{O}$ (40% by weight) at 60°C constant temperature for 12 h. The micromachined samples were then immersed in a reflux system containing concentrated phosphoric acid at 140°C for 2 h in order to remove the silicon nitride and then in a buffered-oxide-etch (BOE 1:20) bath for 10 min to remove the thermal oxide. The samples were rinsed with deionized H_2O and blow dried with nitrogen gas.

Three sets of microstructures were fabricated for this study. All three test structures have etched silicon micromachined V grooves. For the second and third structures, a $1\text{-}\mu\text{m}$ -thick thermal oxide was grown at 1100°C on the surface of the silicon V-groove samples. A $0.3\text{-}\mu\text{m}$ -thick PECVD nitride was deposited on the thermal oxide of the second structure and $0.5 \mu\text{m}$ of sputtered chromium was deposited on the thermal oxide of the third structure. These test structures provide information on the interaction between the microballs and semiconductor, metallic

TABLE I. Measured and calculated values of friction for silicon/stainless-steel contacts for (a) left to right direction, (b) right to left direction, and (c) average of (a) and (b). The data for θ in (a) and (b) are the average of ten measurements.

Applied load (g)	(a)					(b)					(c)				
	0	5	10	20	50	0	5	10	20	50	0	5	10	20	50
θ°	3.03	0.91	0.71	0.60	0.56	3.38	0.79	0.59	0.58	0.41	3.21	0.85	0.65	0.59	0.49
S.D. ^a	1.15	0.17	0.11	0.13	0.04	1.22	0.15	0.20	0.15	0.09	1.19	0.16	0.16	0.14	0.07
F_N (g)	0.360	5.360	10.360	20.360	50.358	0.360	5.360	10.360	20.360	50.360	0.360	5.360	10.360	20.360	50.360
F_T (g)	0.019	0.085	0.128	0.213	0.492	0.021	0.074	0.107	0.206	0.360	0.020	0.080	0.118	0.210	0.426
$\mu = F_T/F_N$	0.0528	0.0159	0.0124	0.0105	0.0098	0.0583	0.0138	0.0103	0.0101	0.0071	0.0560	0.0149	0.0114	0.0103	0.0085

^aStandard deviation.

TABLE II. Measured and calculated values of friction for silicon nitride/stainless-steel contacts for (a) left to right direction, (b) right to left direction, and (c) average of (a) and (b). The data for θ in (a) and (b) are the average of ten measurements.

Applied Load (g)	(a)					(b)					(c)				
	0	5	10	20	50	0	5	10	20	50	0	5	10	20	50
θ°	1.62	0.91	0.82	0.68	0.58	1.67	0.87	0.80	0.60	0.51	1.65	0.89	0.81	0.64	0.55
S.D. ^a	0.30	0.12	0.36	0.07	0.16	0.35	0.14	0.14	0.12	0.08	0.33	0.13	0.25	0.10	0.12
F_N (g)	0.310	5.309	10.309	20.309	50.307	0.310	5.309	10.309	20.309	50.308	0.310	5.309	10.309	20.309	50.308
F_T (g)	0.009	0.084	0.148	0.241	0.509	0.009	0.081	0.144	0.213	0.448	0.009	0.083	0.146	0.227	0.479
$\mu = F_T/F_N$	0.0290	0.0158	0.0144	0.0119	0.0101	0.0290	0.0153	0.0140	0.0105	0.0089	0.0290	0.0156	0.0142	0.0112	0.0095

^aStandard deviation.

and insulator materials. The thermal oxide serves as an electrical insulation layer when the structure is used as a linear actuator. The friction of all three structures is measured in contact with the stainless-steel microballs.

B. Test setup

The coefficients of friction for silicon/stainless steel, silicon-nitride/stainless-steel, and chromium/stainless-steel contacts at the onset of motion were found by measuring the inclined angle at which the slider of the linear displacement element starts to move. The coefficient of friction is equal to the tangent of the angle at this condition. Prior to measurement, samples were rinsed with deionized water and blow dried with nitrogen gas. Eight stainless-steel microballs were positioned in each of the two silicon micromachined V grooves of the lower plate. This configuration was selected to represent a conventional configuration commonly used in linear bearings. It takes into consideration over constraint due to the use of two grooves as well as any maldistribution of load due to elastic deformations and differential slip caused by four-point contact. The slider of the linear displacement element was aligned with the bottom plate through both V groove races. A tilting table with 1/100 of a degree accuracy was positioned on a precision granite plate. The linear displacement element was positioned on the middle of the tilting table. The table was tilted at increments of 1/10 of a degree. The tilting was stopped once the movement of the slider was observed. Twenty measurements were made for each test structure. This included ten left to right and ten right to left directions. Loads of 5, 10, 20, and 50 g were then applied by placing weights at a marked position on the

linear displacement element. These loads were considered to determine the effect of normal forces on the coefficient of friction.

III. RESULTS AND DISCUSSION

The frictional resistance force F_T and the nominal coefficient of friction μ at the onset of movement for silicon/stainless-steel, chromium/stainless-steel, and silicon nitride/stainless-steel contacts were calculated from the tilt table angle measurements. All measurements were made at room temperature. The average tangential force at the onset of movement is

$$F_T = W \sin \theta, \quad (1)$$

where θ is the inclination angle causing movement and W is the applied force. Note that W is the mass of the upper plate and any additional added weight. The corresponding normal load is calculated as

$$F_N = W \cos \theta. \quad (2)$$

The nominal coefficient of friction at the onset of motion is calculated as

$$\mu = F_T/F_N = \tan \theta. \quad (3)$$

Tables I, II, and III summarize the test results for silicon/stainless steel, silicon nitride/stainless steel, and chromium/stainless steel, respectively. Each table shows the results of (a) left to right measurements, (b) right to left measurements, and (c) average of (a) and (b). θ° is the angle at which the slider moves. The values in parts (a)

TABLE III. Measured and calculated values of friction for chromium/stainless-steel contacts for (a) left to right direction, (b) right to left direction, and (c) average of (a) and (b). The data for θ in (a) and (b) are the average of ten measurements.

Applied load (g)	(a)					(b)					(c)				
	0	5	10	20	50	0	5	10	20	50	0	5	10	20	50
θ°	1.56	0.75	0.59	0.54	0.46	1.10	0.83	0.63	0.53	0.49	1.33	0.79	0.61	0.54	0.48
S.D. ^a	0.26	0.16	0.18	0.12	0.05	0.30	0.17	0.17	0.16	0.09	0.28	0.17	0.18	0.14	0.07
F_N (g)	1.450	6.450	11.450	21.450	51.450	1.450	6.450	11.450	21.450	51.450	1.450	6.450	11.450	21.450	51.450
F_T (g)	0.040	0.084	0.118	0.202	0.413	0.028	0.093	0.126	0.198	0.440	0.034	0.089	0.122	0.200	0.427
$\mu = F_T/F_N$	0.0276	0.0130	0.0103	0.0094	0.0080	0.0193	0.0144	0.0110	0.0092	0.0086	0.0235	0.0137	0.0107	0.0093	0.0083

^aStandard deviation.

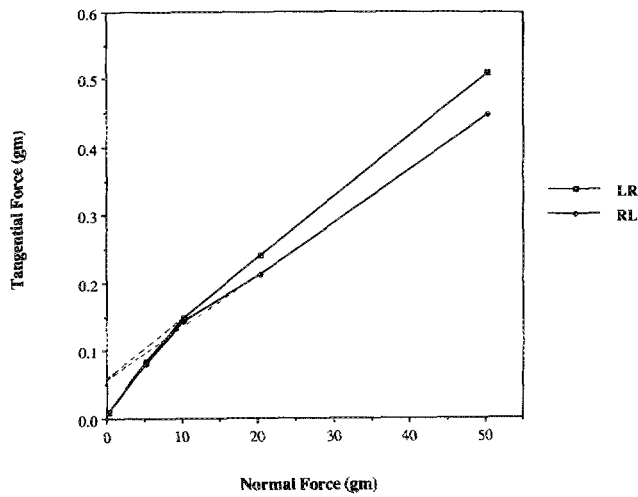


FIG. 3. Tangential force vs normal force for silicon nitride/stainless steel contacts for both left to right and right to left directions. Each point in the graph is the average of 10 measurements. The extrapolated lines coincide at the same point (0.06 g).

and (b) for θ° are the average of ten measurements and a standard deviation is provided. Results are given for applied loads of 0, 5, 10, 20, and 50 g.

A sample plot of the average tangential force versus the normal load at the onset of rolling motion for the silicon nitride/stainless steel material is given in Fig. 3. Both left to right and right to left motions are provided. It can be seen that the frictional resistance at the higher normal loads is approximately 10% greater for the left to right than the right to left motion. This difference may be attributed to the micromachining process or the variable conditions at the initial location of the slider. The values of F_T at the lower normal loads are essentially the same. It can also be seen that the extrapolated value for F_T at $F_N = 0$ (which can be considered as the theoretical adhesive resistance) is equal to 0.06 gm in this case and is the same for both directions of motion.

Figure 4 shows a comparison between the average values for the frictional resistance at the onset of rolling in both directions of motion for the considered three materials. It can be seen that all three materials exhibit similar behavior and the results can be expressed by the following equations:

$$F_T = 0.046 + 0.0076F_N \quad (\text{silicon/stainless steel}), \quad (4)$$

$$F_T = 0.059 + 0.0083F_N \quad (\text{silicon nitride/stainless steel}), \quad (5)$$

$$F_T = 0.036 + 0.0076F_N \quad (\text{chromium/stainless steel}) \quad (6)$$

for normal loads greater than 10 g. It is interesting to note that the average values for the extrapolated adhesive resistance (F_T at $F_N = 0$) are 0.046, 0.059, and 0.036 for the silicon/stainless steel, silicon nitride/stainless steel, and chromium/stainless steel, respectively.

A plot of the average nominal coefficient of friction (F_T/F_N) for all three materials is shown in Fig. 5 as a

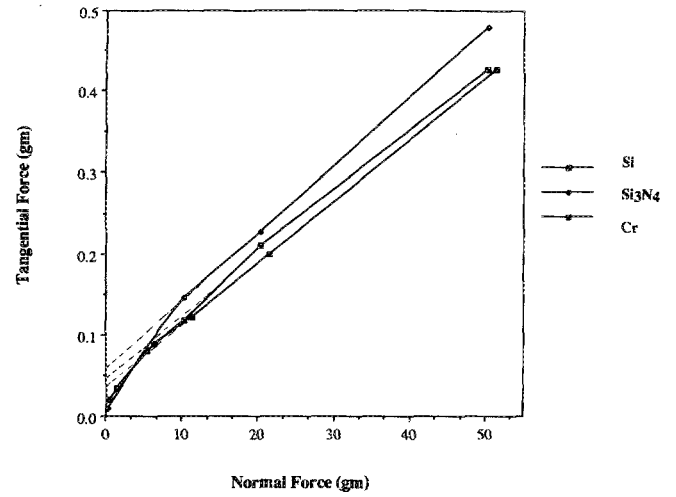


FIG. 4. Tangential force vs normal force for all three test specimens. The data represent an average of 20 measurements. The extrapolated lines show the theoretical values of the tangential force for all three cases on the vertical axis.

function of the normal load. It can be seen that due to the adhesive component of the frictional resistance, the coefficient of friction is relatively high when the slider rolls without any added normal load (under its own weight). The averaged value at zero added force for both directions of motion is 0.0560 for silicon/stainless steel, 0.0290 for silicon nitride/stainless steel, and 0.0235 for chromium/stainless steel. The asymptotic values for the average coefficient of friction (at very high normal loads) are 0.0076, 0.0083, and 0.0076 for the three materials, respectively.

IV. CONCLUSIONS

This article presents results on the tangential forces necessary to initiate rolling motion of stainless-steel microballs in micromachined silicon V grooves with and without deposited thin films. The use of a tilting table with 0.01°

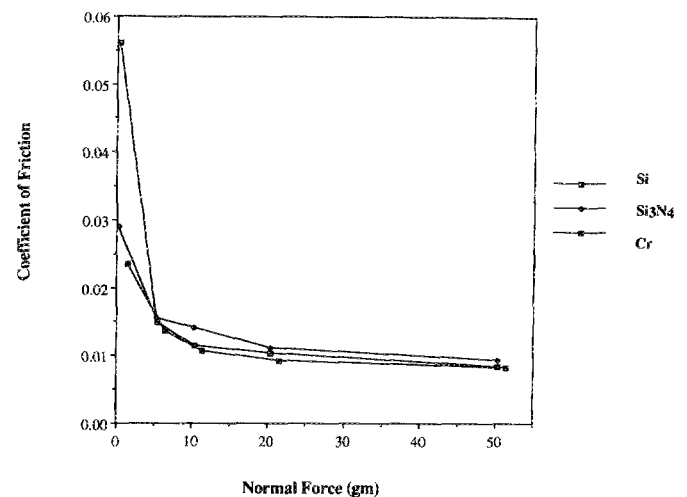


FIG. 5. Coefficient of friction vs normal force for all three test specimens. The data represent an average of 20 measurements.

incremental movement proved useful in generating reliable data on the frictional resistance at the onset of rolling for the considered rolling models. The coefficients of friction reported here are significantly lower than the published data on sliding friction in micromotors or microactuators as would be expected. This article provides the baseline information necessary for the design and optimization of MEMS using rolling bearings with the conventional two groove structures.

ACKNOWLEDGMENTS

The authors would like to thank Daniel C. Christensen, manager of the Wisconsin Center for Applied Microelectronics and Robert J. Sandberg, director of Mechanical Engineering Central Service Shop at the University of Wisconsin-Madison for their technical suggestions. This

work was supported in part by the National Science Foundation in the form of Denton's Presidential Young Investigator Award (Ref. No. ECS-8657655).

- ¹Y. C. Tai and R. S. Muller, *Sensors Actuators A21-A23*, 180 (1990).
- ²M. G. Lim, J. C. Chang, D. P. Schultz, R. T. Howe, and R. M. White, in *Proceedings of IEEE Workshop on Micro Electro Mechanical Systems*, Napa Valley, CA, February, 1990 (IEEE, New York, 1990), p. 82.
- ³M. Mehregany, S. D. Senturia, and J. H. Lang, in *Technical Digest of IEEE Solid State Sensors and Actuators Workshop*, Hilton Head Island, SC, June, 1990 (IEEE, New York, 1990), p. 17.
- ⁴K. Noguchi, H. Fujita, M. Suzuki, and N. Yoshimura, in *Proceedings of the IEEE Workshop on Micro Electro Mechanical Systems*, Nara, Japan, February, 1991 (IEEE, New York, 1991), p. 148.
- ⁵S. Suzuki, T. Matsuura, M. Uchizawa, S. Yura, H. Shibata, and H. Fujita, in Ref. 4, p. 143.
- ⁶K. Deng and W. H. Ko, *J. Micromech. Microeng.* 2, 14 (1992).
- ⁷Thomson Precision Ball Company, Inc., Bristol, CT 06010.